Revista de la Academia Colombiana de Ciencias Exactas, Físicas y Naturales.
47(182):37-50, enero-marzo de 2023. doi: https://doi.org/10.18257/raccefyn.1821

Physical Sciences

Original article

Estimation of suitable upper-limits for temperature, in stability comparisons between solid phases at high pressures. Study cases: carbon, oxygen, and fluorine

Estimación de valores máximos razonables de temperatura, para comparaciones de estabilidad entre fases sólidas a altas presiones. Casos de estudio: carbono, oxígeno y flúor

Javier A. Montoya*, Beatriz H. Cogollo-Olivo

[1] Instituto de Matemáticas Aplicadas, Universidad de Cartagena, Cartagena de Indias, Colombia

Inaugural article for admission of Javier A. Montoya, as correspondent member of the Colombian Academy of Exact, Physical and Natural Sciences

Abstract

For most solid materials the Quasi-Harmonic Approximation (QHA) is expected to stay valid in a wide range of temperatures that get extended as we increase pressure, reaching a limit that could vastly exceed the melting temperature of the material. Hence, it becomes relevant to develop additional criteria for constraining the maximum temperature under which it still makes sense to perform stability comparisons between crystalline phases, hopefully without paying the high computational price that is required to calculating the precise melting curve for each solid phase. In this work, we report that for crystalline systems in which QHA remains accurate at high temperature, an alternative and computationally inexpensive phenomenological approximation holds well for identifying the region in the pressure-temperature (P-T) space where melting is likely to occur, meaning, the Lindemann's criteria. By quantifying how atoms deviate from their equilibrium positions upon increasing temperature in the solid phase, we were able to constrain their P-T region of stability to conditions that are located under a line that represents an 11% average deviation of the atoms with respect to their interatomic distances, therefore, providing an approximate but reliable lower limit for the melting line which is relatively easy to calculate, and also a very useful alternative when no accurate experimental data is available and calculations do not exist or are not conclusive.

Keywords: Lindemann; Melting; DFT; QHA; High Pressure; Diamond.

Resumen

En sólidos, la aproximación cuasi-armónica tiende a ser válida en un amplio rango de temperaturas, que aumenta conforme se aplica mayor presión al sistema y su máximo puede exceder ampliamente la temperatura de fusión. Cobra entonces relevancia desarrollar criterios que restrinjan la temperatura bajo la cual es razonable realizar comparaciones teóricas de estabilidad entre fases sólidas, sin incurrir en los altos costos computacionales necesarios para el cálculo preciso de la línea de fusión de cada una de ellas. Aquí reportamos que para cristales presurizados donde la aproximación cuasi-armónica es bastante confiable, el criterio fenomenológico de Lindemann es idóneo para estimar eficientemente las condiciones de presión y temperatura donde es probable que ocurra la transición desde las fases sólidas hacia el líquido. Cuantificando la desviación promedio de los átomos desde sus posiciones de equilibrio conforme aumenta la temperatura, en carbono a muy alta presión, fue posible determinar que la región de estabilidad de la fase sólida se circunscribe a una región del espacio de presión y temperatura ubicada bajo la curva que representa el 11% de desviación promedio de los átomos con respecto a las distancias interatómicas del material. Lo anterior proporciona un criterio aproximado pero confiable para sugerir el valor máximo de estabilidad de sólidos presurizados, el

Citation: Montoya JA, Cogollo-Olivo BH. Estimation of suitable upper-limits for temperature, in stability comparisons between solid phases at high pressures. Study cases: carbon, oxygen, and fluorine. Revista de la Academia Colombiana de Ciencias Exactas, Físicas y Naturales. 47(182):37-50, enero-marzo de 2023. doi: https://doi.org/10.18257/raccefyn.1821

Editor: María Elena Gómez de Prieto

***Corresponding autor:**
Javier A. Montoya;
jmontoyam@unicartagena.edu.co

Received: November 21, 2022
Accepted: December 26, 2022
Published on line: February 24, 2023

Revista de la Academia Colombiana de Ciencias Exactas, Físicas y Naturales.
47(182):37-50, enero-marzo de 2023. doi: https://doi.org/10.18257/raccefyn.1821

cual es relativamente simple de calcular representando al mismo tiempo una opción atractiva si no existen datos experimentales ni cálculos teóricos de fusión, o si estos no son concluyentes, situación que se aprovechó aplicando el criterio a los sistemas de oxígeno y flúor.

Palabras clave: Lindemann; Fusión; DFT; Cuasi-Armónico; Alta Presión; Diamante.

Introduction

Phase diagrams of simple pure substances at extreme pressure and temperature (P-T) are of great interest for understanding the internal conditions of planets in our solar system and in exoplanets. From a purely fundamental point of view, the study of the stability of atomic structures and the behavior of the electronic clouds inside simple materials upon changes in pressure and temperature, can help scientist to build a deeper understanding of the quantum mechanical nature of matter and its practical implications. In recent years, our research group has studied the high P-T phase diagrams of carbon (**Cogollo-Olivo**, 2020), oxygen (**Cogollo-Olivo *et al.,*** 2018), and one of their mixtures: CO_2 (**Cogollo-Olivo *et al.,*** 2020). Carbon dioxide was studied theoretically within a region of pressures that is currently dominated experimentally by the Diamond Anvil Cell (DAC) technique (**Loveday**, 2012). DAC is the most favored technique for studies of matter starting at pressures around 5 Giga-pascals (GPa) and reach values that exceed by far the maximum pressure achievable by large-volume hydraulic-presses, since DAC's pressure range can extend up to several hundredth GPa. As a matter of fact, nowadays it's not too challenging to obtain reliable measurements for physical properties of matter from samples compressed up to 200 GPa, although, also pressures of 750 GPa and above have been reported by compressing noble metals such as osmium and rhenium (**Dubrovinsky *et al.,*** 2015; **Dubrovinskaia *et al.,*** 2016). Regarding finite temperature studies, DACs can be fitted inside cryostats to study the behavior of matter under high pressure and very low temperature (**Somayazulu *et al.,*** 2019), while, for high temperature studies, a conventional resistive heating device can be attached to the DAC to produce very precise temperatures that can go up to a few thousand Kelvin at the location of the sample (**Santoro *et al.,*** 2020). Much higher temperatures can also be reached by laser-heating techniques, where the temperature of the sample is determined close to the heated spot from the light emitted using a black-body radiation model and also calculating its decay across the heated sample from known values for the thermal conductivity of the sample, to infer its temperature at places away from the laser heating spot according to the calculated thermal gradient (**Goncharov *et al.,*** 2009; **Montoya & Goncharov**, 2012). Even with all these outstanding experimental advances for measuring the properties of matter at relatively high P-T conditions, CO_2 remained very challenging to describe in a region with pressure going from 10 to 50 GPa and temperatures from 0 to 2000 K, which is comfortably within the access of current DAC implementations. The observed uncertainties in CO_2's phase diagram were not due to limitations on the experimental techniques at said P-T conditions, they existed, instead, due to this molecule's nature itself. CO_2 forms very stable molecular solid phases that are difficult to reconfigure into new ones, even after reaching conditions where the previous phase is no longer stable. The theoretical work that was done at our group was key for clarifying previous misconceptions related to the real thermodynamic regime of stability for each experimentally reported crystalline form. We achieved this by comparing their enthalpies at 0 K, including also the zero-point energy, and performing stability comparisons between solid phases that included finite temperature contributions to the Helmholtz free energy, calculated within the Quasi-Harmonic-Approximation (QHA), allowing us to construct also the Gibbs free energy of the system (**Cogollo-Olivo *et al.,***2020). This last statement begs the question: Up to what temperature is it still meaningful to compare free energies between solid crystalline phases? On a first approach, the answer to this question is two-fold, first, there is the aspect related to the P-T conditions of validity for the technique that is used to calculate the temperature contributions to the free energy and, second, there is the aspect of the temperature limit for

which a substance stops having a solid form and moves towards melting. As an example of the first aspect just mentioned, a calculation of the Debye temperature (Θ_D) for CO_2's molecular forms was performed, because it is a commonly accepted rule that increasingly relevant contributions coming from anharmonicities usually start to appear at temperatures around or higher than $1.2\Theta_D$ (**Baroni *et al.,*** 2010; **Angel *et al.,*** 2019), therefore, it seems relevant to estimate this temperature limit when using non-anharmonic treatments such as QHA. Luckily, the limit of validity for the QHA treatment usually moves higher in temperature upon increasing pressure (**Baroni *et al.,*** 2010; **Angel *et al.,*** 2019; **Anderson**, 1995). As a concrete example, the $1.2\Theta_D$ limit had values between 3485 K and 3500 K for all the molecular forms of CO_2 that we considered in our previous study, even at their lowest pressure (10 GPa), implying that 3485 K would be a reasonable upper limit for the temperature in the entire pressure range of our study (**Cogollo-Olivo *et al.,*** 2020). However, considering the second aspect of the answer given earlier regarding melting, even if our last statement suggested that for CO_2 one could keep comparing solid phases up to $1.2\Theta_D$ in order to find out which one gets stabilized due to entropy contributions within QHA, it is worth noticing that if the experimental evidence for melting is taken into account it doesn't make any sense to go above 800 K in our solid vs. solid calculations. Therefore, in the current work we will care about determining the conditions for melting, since, as we will see, at high pressures the transition towards the liquid often occurs at temperatures that are well within QHA's limit of validity.

Besides being the major constituent of CO_2, oxygen is very interesting in its own right, for example, in its molecular form O_2 exhibits a very rich phase diagram and a variety of electronic properties, going from being an insulator (**Crespo *et al.,*** 2014) to becoming a metal (**Akahama *et al.,*** 1995), then an antiferromagnet (**Nicol *et al.,*** 1979; **Schiferl *et al.,*** 1983; **Gorelli *et al.,*** 2002; **Goncharenko *et al.,*** 2004), and finally a superconductor (**Ma *et al.,*** 2007; **Weck *et al.,*** 2009). Apart from that variety of properties, which have been experimentally observed at pressures between 0 and 130 GPa, oxygen also shows an interesting behavior due to a strong lone-pair repulsion in its extended solid forms, that become more stable than its molecular forms at Tera-pascal (TPa) pressures (**Sun *et al.,*** 2012; **Cogollo-Olivo *et al.,*** 2018). Oxygen offers an example of a situation where the crude extrapolation of its melting line, based on theoretical and experimental data, yields the unrealistic melting temperature of 26000 K around 2 TPa (**Weck *et al.,*** 2007; **Goncharov *et al.,*** 2011). This is so, because no direct data has been obtained close to those extreme conditions and the referred extrapolation is based on data below 100 GPa that can, therefore, be very inaccurate at much higher pressures. Still, this crude estimation provided a reasonable justification for assessing the relative stability between solid phases of oxygen a TPa pressures by comparing their free energies within QHA at temperatures going up to 8000 K (**Cogollo-Olivo *et al.,*** 2018), showing that within that temperature range two previously unknown triple points between solid phases can be found and it still remains to see if they can be detected experimentally.

Although the behaviour of oxygen at TPa pressures remains interesting and open to further study, the results contained in our present work are supported by evidence obtained when analyzing the other constituent element of CO_2, *i.e.*, carbon. This element is nonmetallic and is also the fourth most abundant element in the universe by mass. Carbon assumes the diamond phase around 10 GPa and stays with it as its most stable phase up to roughly 1 TPa. Recognized as a "miracle material" due to its well-known outstanding thermal conductivity, transparency, hardness, overall mechanical stability, and interesting properties upon the introduction of selected impurities, diamond is very relevant for current and future technological applications in industry and society. In astrophysics, diamond has been predicted to exist in massive amounts within the interior of some gas giants in our solar system (**Ross**, 1981), as well as in the interior of large extra-solar planets where carbon is expected to reach also post-diamond solid phases due to extreme pressures. It is not surprising then, that due to its importance and wide range of stability, diamond has become the archetype of a mono-atomic covalent solid and has been extensively studied

Revista de la Academia Colombiana de Ciencias Exactas, Físicas y Naturales.
47(182):37-50, enero-marzo de 2023. doi: https://doi.org/10.18257/raccefyn.1821

under extreme conditions to pursue a fundamental understanding of matter. The limits to diamond's stability and its overall behaviour have always been tested with state-of-the-art experimental techniques, therefore, as soon as a new method for applying higher pressures is developed diamond is always a forefront candidate to apply said method. Hence, the recently developed ramp-compression shock-wave technique, which borrows technological developments from high power laser facilities that were built to achieve nuclear fusion by compressing hydrogen, has been no exception to diamond's appeal (**Smith *et al.,*** 2014; **Swift *et al.,*** 2022). Also, being of high interest for theoretical studies, it is known that atomistic simulations produce two main post-diamond stable phases at low temperatures, *i.e.*, BC8, which has a small electronic band-gap when compared to diamond's but is still covalent (**Grumbach & Martin**, 1996; **Correa *et al.,*** 2006; **Correa *et al.,*** 2008; **Martinez-Canales *et al.,*** 2012; **Benedict *et al.,*** 2014) and a simple cubic (SC) phase, which is metallic (**Martinez-Canales *et al.,*** 2012; **Benedict *et al.,*** 2014). In this system, same as for oxygen, the enormous pressures that are involved in the study of carbon's solid-liquid interface close to its transition from diamond to BC8, make it very challenging to get an accurate estimation for the melting curve purely by extrapolating available experimental data (**Alder & Christian**, 1961; **Bundy**, 1980). Several attempts to determine the melting line of carbon at very high pressures have also been made theoretically (**Grumbach & Martin**, 1996; **Wang *et al.,*** 2005; **Correa *et al.,*** 2008; **Benedict *et al.,*** 2014; **Schöttler *et al.,*** 2016), but due to lack of consistency in the results there is no consensus on the theoretical melting lines existing up to this date.

Although no detailed analytical model explaining the melting temperature exists, we estimated a region for carbon's solid-to-liquid transition based on a purely phenomenological vibrational approach known as the Lindemann's criteria, which considers only the properties of the solid phase. Following Einstein's model of a solid made of harmonic oscillators arranged in a simple cubic lattice, the original formulation of this criteria relied on the assumption that the atomic vibrations in the solid could be represented just in terms of its Debye frequency at high enough temperature. Therefore, in the way it was originally stated, the criteria use macroscopic knowledge to calculate a quantity known as the Lindemann's ratio (L), in terms of the temperature of the system, the atomic mass number, its volume, and the Debye temperature. This ratio, presented in Lindemann's original work just as a proportionality constant, was believed to reach an universal critical value for all materials at melting (**Grüneisen**, 1926), derived from the assumption that at the transition temperature towards the liquid phase the amplitude of the thermal displacements due to the oscillation of the atoms would reach one-half the inter-atomic distance less the atom's diameter, allowing direct contact between neighboring atoms (**Lindemann**, 1910). Later, it became evident that the atomic displacements at melting were not that large and also the universality didn't seem to hold, instead, actual values of L coming from experimental data and simulations for simple systems spanned a range going from 0.05 to 0.2 depending on factors such as crystal structure, nature of inter-particle interactions, and magnitude of quantum effects, among others (**Chakravarty *et al.,*** 2007). Still, the original assumption was not completely wrong, since this classic formulation done by Lindemann has been be found recently to predict melting temperatures at ambient pressure with an uncertainty lower than 22 % for 39 simple systems, by using an exact same value of L, which is of the order of 0.1, for each element belonging to a given group of the periodic table (**Vopson *et al.,*** 2020). This establishes L, at present, as the only available predictive phenomenological tool for understanding solid-liquid coexistence conditions for a range of metals and geologically important minerals with very high melting temperatures. In fact, there are connections between Lindemann's relation and other well established theories, suggesting that it could be more than just a semi-empirical rule (**Gilvarry**, 1956; **Ross**, 1969).

Nowadays, the most widely adopted definition of Lindemann's criteria is the reformulation provided by Gilvarry (**Gilvarry**, 1956), who presented a description of this criteria relating it directly to microscopic quantities taken from the vibrational response of the

system at finite temperature, demonstrating that for a crystalline phase *L* is the fraction between the root-mean-squared displacement of the atoms and the inter-atomic spacing at a given temperature. Gilvarry also suggested that this ratio should be universal if the main assumptions of the models behind its estimation stay valid, meaning, within a sub-category of well-behaved isotropic mono-atomic solids. In fact, previous works using Lindemann's criteria were expected to be inexact by design and they could hope at best only for an approximate agreement between theory and experiment. For example, they had limited resources available for performing complex calculations and in some cases had to restrict the available frequencies and the orientations of the vibrational modes in the solids, or calculated those together with the inter-atomic distances using approaches from classical mechanics that were limited by the type of structural ordering considered or the interatomic potential used, such as Lennard-Jones and its variants, Gaussian core model, inverse-power potentials, etc. On the other hand, the hard-sphere system represents the simplest nontrivial liquid with a freezing transition, and is thus the prototype of a model for nearly spherical closed-shell atoms or molecules, where theories and simulations of freezing can directly be compared and have offered consistent values for *L* between theory, simulations, and experiments, being this system where density functional theory has had a notable success (**Löwen**, 1994). First principle calculations offer essentially a test for the theory of the solid state because of their high accuracy, in this context Lindemann's melting rule has been obtained from first principles for real materials in the past (**Stroud & Ashcroft**, 1972; **Bilgram**, 1987), finding values for its ratio around 0.13, which coincide almost exactly with first principles values of *L* obtained for the melting of hard-sphere solids (**Young & Alder**, 1974; **Ohnesorge *et al.,*** 1993; **Murray & Grier**, 1996), failing only for extremely soft potentials that would imply long range microscopic interactions (**Löwen**, 1994). Also at ambient pressure, others have reported this criteria to work very well for rare gases and mono-atomic metals, in particular the alkali ones, which are composed of spherical or nearly spherical units that are characterized predominantly by two-body central bonding forces (**Bilgram**, 1987). A successful application of the criteria at ambient pressure excludes so far radioactive elements, rare-earths, and semiconductor elements (**Vopson *et al.,*** 2020). Here, for our dense and highly symmetric mono-atomic materials under extreme conditions, we do not consider heavy elements, surface effects, nor lattice defects, also, the pressures considered are so high that metallization occurs or is close to occur in all our studied crystalline phases, making long range interactions far from being predominant and removing most of the divergences from an idealized hard-sphere model.

Summarizing, in this work, avoiding the computational sophistication involved in finding a very precise melting curve, we attempt to locate the maximum temperature for three solid phases of diamond up to which meaningful stability comparisons between them can be made at TPa pressures, by testing the Lindemann's criteria (**Lindemann**, 1910; **Gilvarry**, 1956) within QHA. We managed to approximate carbon's melting temperature quantitatively and the shape of its melting line with high certainty and at a relatively low computational cost, being then able to suggest a limiting value for *L* corresponding to the temperature above which melting is most likely to have already occurred for most, if not all, materials under extreme conditions. The hypothesis of a close-to-universal *L* was then applied to the cases of oxygen and fluorine, where no direct experimental or theoretical data is available for melting conditions at TPa pressures. The use of QHA for this purpose is well justified, since it is not unusual that the elastic properties of a crystalline solid remain well behaved right up to its melting point (**Hunter**, 1942), therefore, developing anharmonicities or a softening of the material is not a prerequisite before melting. As a matter of fact, these so called "catastrophe hypotheses" about mechanical properties hinting towards lattice instability before melting, would be incompatible with the existence of super-heated crystals (**Bilgram**, 1987). Instead, it has been proposed that a more accurate hypothesis for the conditions leading to melting, from a first principles perspective, seems

Revista de la Academia Colombiana de Ciencias Exactas, Físicas y Naturales.
47(182):37-50, enero-marzo de 2023. doi: https://doi.org/10.18257/raccefyn.1821

to be the disappearance of the nucleation barrier at the surface of the material due to an increase of the root-mean-square amplitude of the thermal vibrations (**Stroud & Ashcroft**, 1972), meaning that using QHA in the application of Lindemann's rule should be a valid approach in most cases.

Materials and Methods

Carbon was examined in the pressure range going from 0.25 to 3.50 TPa, which includes diamond as well as two post-diamond phases, BC8 and SC. To obtain the structural parameters for all the studied phases, we performed variable-cell optimization calculations at steps of 0.25 TPa within Density Functional Theory (DFT) (**Giannozzi *et al.,*** 2009, 2017), using a projector augmented wave pseudopotential (**Blöchl**, 1994) with six explicit electrons per atom. In this work, the Perdew-Burke-Ernzerhof (PBE) Generalized Gradient Approximation (GGA) of the exchange-correlation functional was used (**Perdew *et al.,*** 1996). To describe electrons, the kinetic energy cutoff of the plane-wave basis set was set to 200 Ry, while, for integrating the first Brillouin-zone with the Monkhorst-Pack method (**Pack & Monkhorst**, 1977), k-point grids of 8x8x8, 4x4x4, and 32x32x32, were used in the cases of diamond, BC8, and SC, respectively, to ensure a converged k-point sampling with similar k-point densities for each size of the unit-cell. These parameters ensured an energy convergence of at least 1 meV/atom.

Finite temperature studies were possible thanks to the calculation of phonon frequencies at zero temperature with harmonic dynamical matrices that were obtained within Density Functional Perturbation Theory (DFPT) in the linear response regime (**Baroni *et al.,*** 2001) with a converged **q**-point grid of 2 ×2 ×2 for diamond and BC8, while 6 × 6 × 6 was used instead for the smaller SC cell. Finite-temperature contributions to the Helmholtz free energy were computed by means of QHA (**Leibfried & Ludwig**, 1961; **Baroni *et al.,*** 2010) from 0 to 10000 K, with the relation:

$$\begin{aligned} F(V,T) &= U_0(V) + \frac{1}{2}\sum_{\mathbf{qs}} \hbar\omega_{\mathbf{qs}} \\ &+ k_B T \sum_{\mathbf{qs}} \ln[1-\exp(-\hbar\omega_{\mathbf{qs}}/k_B T)], \end{aligned} \quad (1)$$

where $\omega_{\mathbf{qs}}$ is the frequency of the mode **s** at point **q** in the Brillouin Zone and a given volume V ; $U_0(V)$ is the ground state electronic energy of the crystal at volume V, and the second and third terms on the right-hand-side of the above equation are the zero-point energy (ZPE) and the thermal vibrational contribution to the free energy, respectively, at volume V. All calculations described so far were performed using the QUANTUM-ESPRESSO package (**Giannozzi *et al.,*** 2009, 2017).

We then fitted the Helmholtz free energy and the volume of each phase at different temperatures to a 3^{rd} order Birch-Murnaghan equation of state, with a variance (χ^2) of order 10^{-5} or better for all fits. With the previous data, the Gibbs free energy was calculated as:

$$G(P,T) = F[V(P,T),T] + PV(P,T). \quad (2)$$

Oxygen and fluorine followed an equivalent treatment. In what follows, if no extra details are given it means that the settings and methods are the same as carbon's, explained above.

For oxygen we selected the two structures that were found to be stable at high temperature in the range of pressure of this study, 1 to 6 TPa: a molecular structure with symmetry $R\bar{3}m$ and a non-molecular structure $Fmmm$. The valence electron wavefunctions were expanded in a plane-wave basis set with a kinetic energy cutoff of 400 Ry. For the primitive cells of the two phases of oxygen considered in this study the size of the k-point grids are 18 × 18 × 18 and 8 × 16 × 16, respectively. When the metallic state was present, the calculations were done using the Fermi-Dirac smearing technique with a width of 43 meV, to account for the electronic entropy at 500 K. This width was kept fixed while calculating the vibrational properties at all temperatures, since this smearing term's

contribution was found to be not very temperature dependent. The vibrational properties for oxygen at $T = 0$ K were also calculated using DFPT and the q-point grids used to obtain the dynamical matrices were as follows: 4 × 4 × 4 for $R\bar{3}m$ and 2 × 4 × 4 for $Fmmm$.

For the solid phases of fluorine, detailed calculations were carried in the same pressure range as for oxygen, with its two most stable structures (**Olson *et al.,*** 2020; **Duan *et al.,*** 2021): *Cmca* and $Pm\bar{3}n$, using a projector-augmented wave pseudopotential with seven explicit valence electrons. The k-point grids for the Brillouin zone integration were also generated using the Monkhorst-Pack method with sizes 16 × 16 × 16 for both *Cmca* and $Pm\bar{3}n$. Other two phases were not included here because their range of stability is restricted to a very narrow region of pressures and, on top of that, the reports about their boundaries with phases *Cmca* and $Pm\bar{3}n$ have been contradictory in previous works.

The Lindemann's ratio was calculated for each solid phase as the fraction between the root-mean-squared displacement for all the atoms at finite temperature and their respective nearest-neighbor distances (**Lindemann**, 1910; **Grüneisen**, 1926; **Gilvarry**, 1956). Therefore, this quantity depends on pressure through the change on the size of the unit cell which in turn depends on its elastic constants, that also characterize the vibrational displacement of the atoms in a solid system due to temperature. Within our current approach, the root-mean-squared displacement and volume for each cell at finite temperature came from the same QHA calculations that were performed previously for generating the Gibbs free energies, hence, the data that was required to produce the Lindemann's ratio came to us at almost zero additional computational effort. An useful reformulation of L in terms of lattice frequencies is provided in Eq. (3) of Ref. (**Pal & Sharma**, 1967).

Results and Discussion

Carbon

In **figure 1**, we present our calculated pressure vs. volume behavior for three relevant carbon phases in the pressure interval going from 0.5 to 3.5 TPa, showing very good agreement between our results and a previous work that also covered the equations of state for diamond, BC8, and SC, which was done by using very accurate pseudopotentials with small core radii and with all six electrons included explicitly (**Martinez-Canales *et al.,*** 2012).

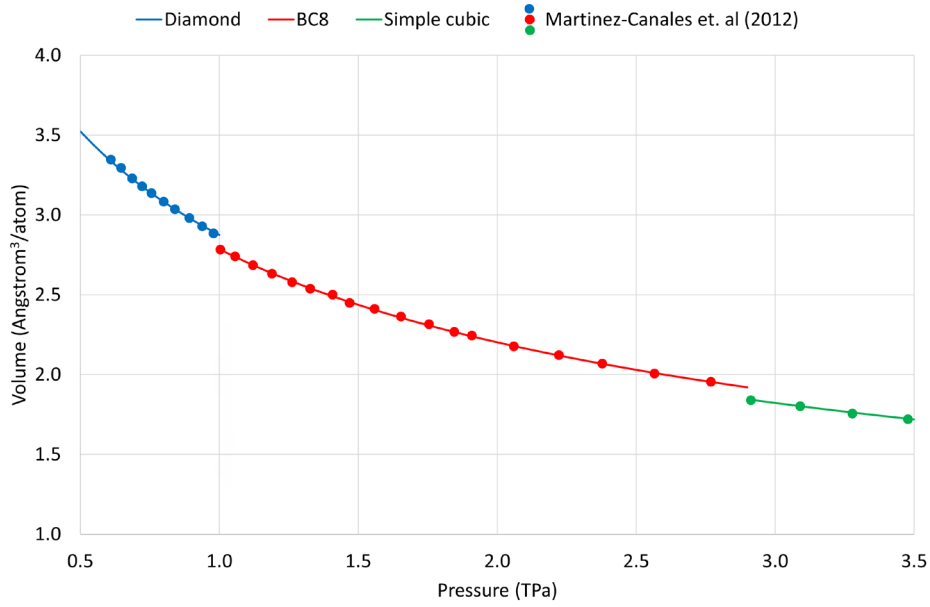

Figure 1. Pressure-volume relation coming from a fit to the 3rd order Birch-Murnaghan equation of state at 300 K for diamond and the two post-diamond phases BC8 and SC. Values extracted from Ref. (**Martinez-Canales *et al.,*** 2012) are displayed with circles for each phase at selected pressures

Revista de la Academia Colombiana de Ciencias Exactas, Físicas y Naturales.
47(182):37-50, enero-marzo de 2023. doi: https://doi.org/10.18257/raccefyn.1821

The phase-boundaries for diamond and post-diamond crystalline forms were calculated using the finite-temperature contribution to the free energy within QHA, as described in the Materials and Methods section. Our findings, vertical lines in green color shown in **figure 2**, are in excellent agreement with those including anharmonic effects performed by (**Schöttler *et al.,*** 2016), which are displayed with black vertical dotdashed lines between the studied solid phases. This suggests that QHA is indeed sufficiently accurate for calculating the most relevant thermodynamic properties in these three solid systems. Gray full vertical lines that are also presented in **figure 2**, correspond to solid-solid boundaries from alternative studies (**Benedict *et al.,*** 2014; **Correa *et al.,*** 2008) that are included here in addition to their calculations of the melting lines, which occupy temperatures above 6000 K and are shown with gray dashed lines in the same figure.

At the highest values within the temperature range of our thermal calculations, carbon is expected to become fluid for all three solid phases according to previous works (**Wang *et al.,*** 2005; **Benedict *et al.,*** 2014; **Correa *et al.,*** 2008) as seen in **figure 3**, therefore, in **figure 2** we show an estimation for the melting lines corresponding to each studied solid form. To this end, using a QHA level of treatment for temperature effects, we computed the P-T conditions required for reproducing pre-established values of L, by following the description given in the Materials and Methods section. The melting lines obtained by assuming different critical values of L are displayed in **figure 2**, where it becomes apparent that at all the considered pressures and also for all crystalline phases, the critical value for L that best describes the transition from solid to liquid in this chemical element seems to be, on average, L =0.13. Meanwhile, a safe range of ratios that cover the discrepancies present in previous calculations of carbon's melting line, mentioned in the introduction, should go from 0.11 to 0.15, since those two values of L limit quite well the P-T region where results from previous theoretical calculations of melting are present (**Wang *et al.,*** 2005; **Benedict *et al.,*** 2014; **Correa *et al.,*** 2008). Let us stress again the fact that all these

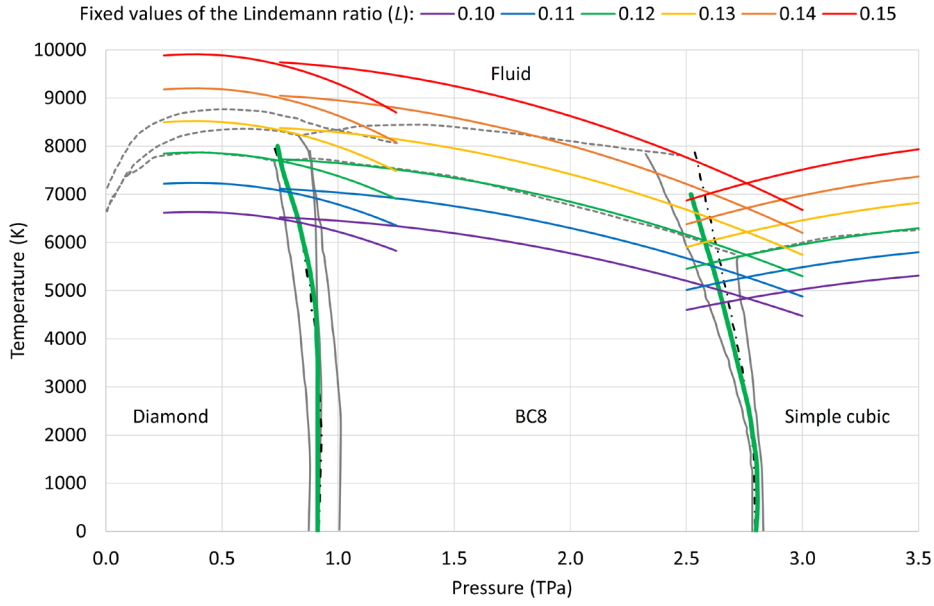

Figure 2. Proposed phase diagram for carbon at extreme conditions including boundaries from previous theoretical works. Our calculated solid-solid phase boundaries (vertical thick green lines) from Ref. (**Cogollo-Olivo,** 2020), fall almost on top of calculations performed by (**Schöttler *et al.,*** 2016) that included small anharmonic corrections, displayed here in black dot-dashed vertical lines and almost covered by our data. Previously reported melting lines for three solid phases of carbon in the TPa regime (gray dashed lines above 6000 K) appear compared against our results (**Cogollo-Olivo,** 2020), which are shown here using lines in a color sequence going from purple to red in the range from L =0.10 to L =0.15, respectively.

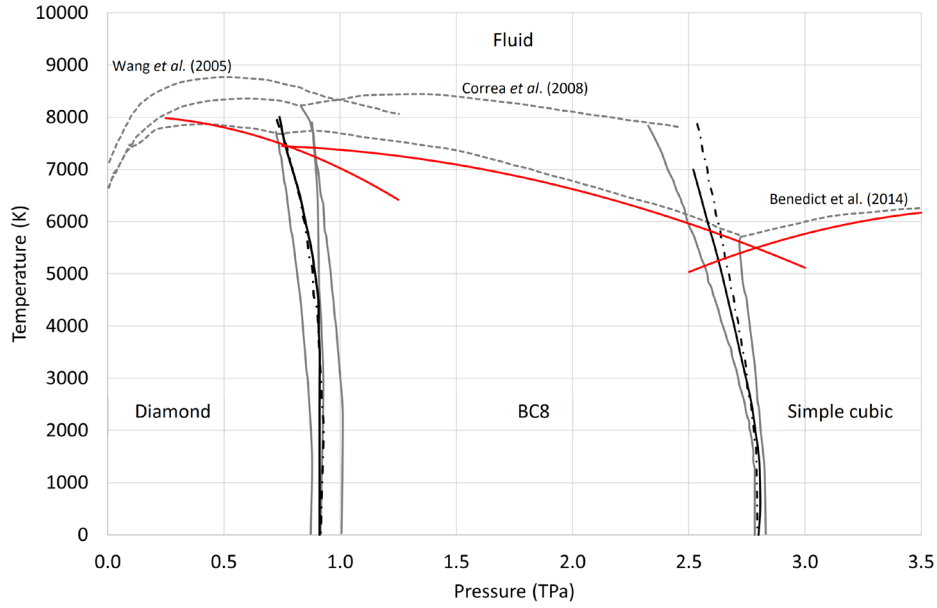

Figure 3. Carbon's melting line estimated using the change in entropy as a criteria, for the three phases in our study.

ratios work consistently well for diamond, BC8, and also for SC, enforcing the idea of L being universal, at least within certain categories of materials and conditions (**Ross**, 1969; **Vopson *et al.,*** 2020). As an additional test, we also considered that at the vicinity of carbon's solid to liquid transition the entropy change has been estimated in the past to lie somewhere between 20 and 30 J·mol/K (**Wang *et al.,*** 2005; **Robinson & Wilson**, 2013). We were then able to calculate a lower limit for the melting line using this criteria, as seen in **figure 3**, seeking a threshold of 20 J·mol/K for the change in carbon's entropy and finding that it coincided quite well with one of our previous approximations, L =1.12 shown in green color in **figure 2**, as well as with previous work (**Benedict *et al.,*** 2014). This additional evidence establishes the Lindemann's criteria as a reliable method to constrain the P-T values taken by melting curves, which, as already mentioned, is also very stable as suggested by the fact that a very similar degree of accuracy in the estimation of the melting lines was obtained simultaneously for diamond, BC8, and the SC phases of carbon, starting from completely independent vibrational studies for each of them.

Oxygen and Fluorine

Encouraged by the previous findings, we now proceed to show the calculation of melting curves for two limiting values for the Lindemann's ratio that were established earlier, L =0.11 and L =0.15, applied to the currently accepted stable phases of oxygen and fluorine, as shown in **figures 4 and 5**.

For oxygen, we can infer that a hypothetical melting line defined by L =0.13, i.e. right in the middle of the range enclosed with blue and red lines depicted in **figure 4**, would clearly stay above all the main interesting features that were presented in the conclusions of our earlier work about different solid oxygen phases (**Cogollo-Olivo *et al.,*** 2018). This newly estimated melting line is far below the one coming from a crude extrapolation of low-pressure data, which gave us a melting temperature of 26.000 K close to 2 TPa. Still, it is worth noticing that even at the lowest melting curve in our range, corresponding to L =0.11, the results of our previous work may stay valid and a triple point could still exist between the solid phases $R\bar{3}m$, *Cmcm*, and *Fmmm* (**Cogollo-Olivo *et al.,*** 2018), within the expected errors, or perhaps it could become a quadruple point, joining these three solid forms with the liquid phase.

Revista de la Academia Colombiana de Ciencias Exactas, Físicas y Naturales.
47(182):37-50, enero-marzo de 2023. doi: https://doi.org/10.18257/raccefyn.1821

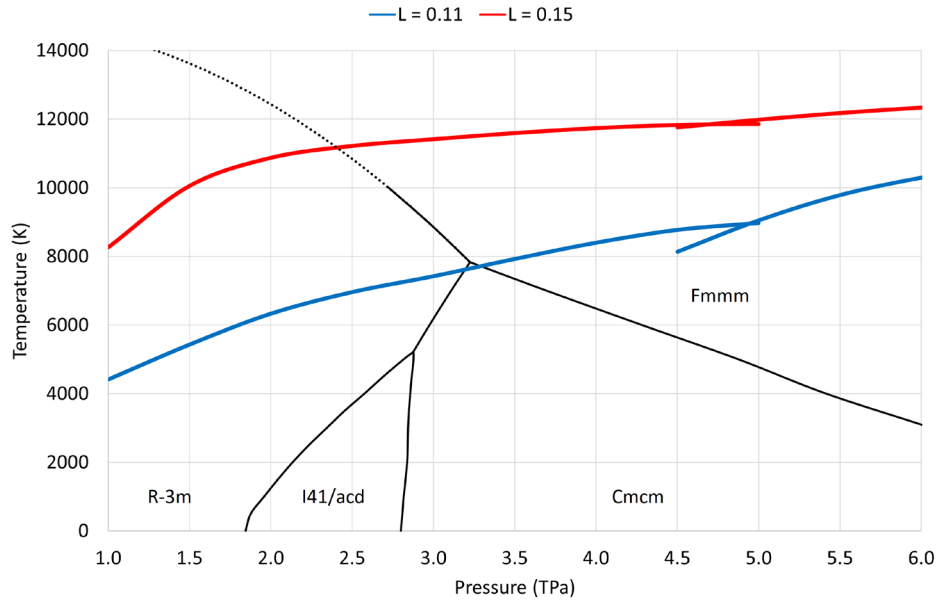

Figure 4. Oxygen's melting region was estimated within the range between L =0.11 and L =0.15, starting from the two most stable solid phases at high temperature, according to previous studies.

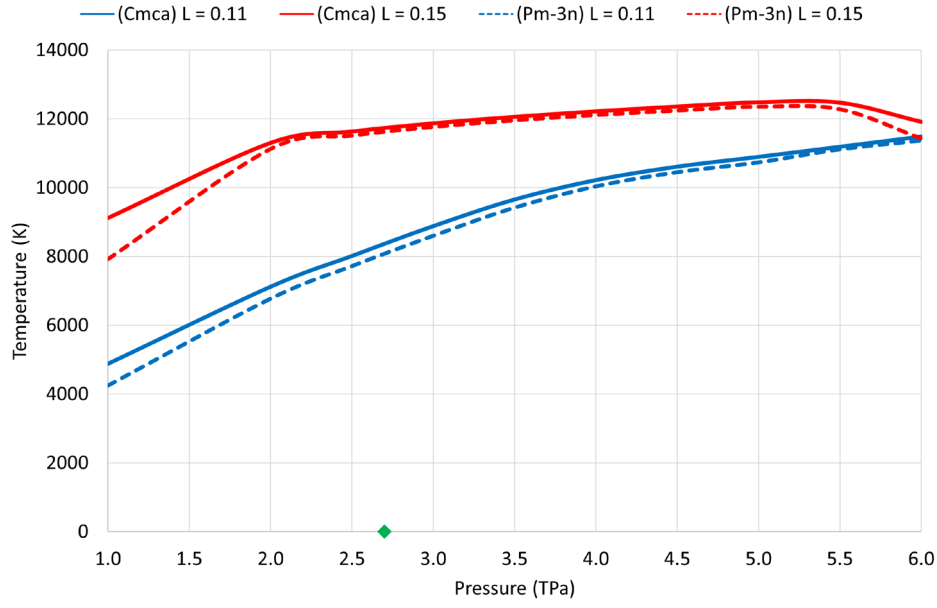

Figure 5. Fluorine's melting region was also estimated in the range between L =0.11 and L =0.15, starting from its two most stable solid phases, according to previous studies.

In the studied pressure range, going from 1 to 6 TPa, same as for oxygen, our melting studies made on fluorine dealt with two widely accepted stable crystalline forms taken from zero temperature studies: *Cmca* and $Pm\bar{3}n$. In terms of structural stability, although belonging to different groups in the periodic table, molecular fluorine closely resembles molecular oxygen due to their closely matching electronegativities, being also the highest in nature. Therefore, it is interesting to see in **figures 4 and 5** that their melting temperatures stayed quite similar in the entire range of pressure conditions, even as extreme as those in this study, and that their behaviors are clearly differentiated from the trend that is followed

by carbon's melting lines. Finally, although almost degenerated, it is important to notice that *Cmca*, full lines in **figure 5**, is more stable than $Pm\bar{3}n$, dashed lines, below 2.7 TPa at zero temperature.

Conclusions

We performed calculations for several carbon phases to identify the P-T conditions that would keep constant the value of Lindemann's ratio (L), which was studied in detail with proposed melting curves in the P-T space that correspond to six fixed values of L in the range from 0.1 to 0.15. We were able to establish that previous attempts at calculating the melting lines for this element can be located with high certainty within a range of L going from 0.11 to 0.15. This allowed us to test the validity of the Lindemann's criteria, which establishes that it is very likely to find the P-T conditions for melting around a single universal value of L. We found that by fixing the ratio to just one of such values (L =0.13) we can represent very well on average all previously calculated carbon's melting lines for its three solid phases considered in this study. L =0.13 is also the value that results from models of hard-sphere solids and provides an outstanding agreement with earlier theoretical estimations that required a much higher computational effort, as well as with an estimation based on the expected changes in entropy across carbon's melting line, for all the solid phases. These findings position the Lindemann's ratio criteria as a robust and computationally inexpensive method to constrain the temperatures at which meaningful comparisons of the relative stability between solid phases should be made, by setting, according to our results for carbon, two limiting values (L =0.11 and L =0.15) as boundaries for a safe estimation on a region in the P-T space under which it makes sense to assume that solid phases can still be present. Finally, since L's definition is not restricted to the use of a particular approximation for obtaining the amplitudes of the atomic displacements as a function of the applied temperature, it may be worth testing Lindemann's criteria using an anharmonic approximation to estimate the atomic displacements in cases where lattice instability is known to exist.

Acknowledgements

JAM and BHC-O are very grateful to Sandro Scandolo for the fruitful discussions about the cases of study cited in this work. To the Abdus Salam ICTP for continuous support, also through the Associates Programme (2020-2025) during the years previous to this work. To the Universidad de Cartagena for its support through internal funds and its HPC facility (ROSMME). Finally, BHC-O wishes to thank MINCIENCIAS for its current support through the "Convocatoria fortalecimiento de vocaciones y formación en CTeI para la reactivación económica en el marco de la postpandemia 2020 - Número 891 de 2020 - Modalidad 2".

Contribution of the authors

JAM: Constructed the driving motivation behind this original contribution, in the terms described in the introduction. ALL authors participated in doing and guiding the calculations, generating the most relevant figures, organizing a comprehensive body of references, analyzing the results and drawing the main conclusions.

Conflict of interests

The authors declare that they do not have any conflict of interest in relation to the content of this work or its financial support.

References

Akahama, Y., Kawamura, H., Haüsermann, D., Hanfland, M., Shimomura, O. (1995). New high-pressure structural transition of oxygen at 96 gpa associated with metallization in a

molecular solid. *Physical Review Letters*, *74*(23), 4690-4693.

Alder, B. J., Christian, R. H. (1961). Behavior of strongly shocked carbon. *Physical Review Letters*, *7*, 367-369.

Anderson, O. (1995). *Equations of state of solids for geophysics and ceramic science*. New York: Oxford University Press.

Angel, R. J., Miozzi, F., Alvaro, M. (2019). Limits to the validity of thermal-pressure equations of state. *Minerals*, *9*(9), 562.

Baroni, S., de Gironcoli, S., Dal Corso, A., Giannozzi, P. (2001). Phonons and related crystal properties from density-functional perturbation theory. *Reviews of Modern Physics*, *73*, 515.

Baroni, S., Giannozzi, P., Isaev, E. (2010). Density-functional perturbation theory for quasiharmonic calculations. *Solid State Physics - Advances in Research and Applications*, *71*, 39-57.

Benedict, L. X., Driver, K. P., Hamel, S., Militzer, B., Qi, T., Correa, A. A., Saul, A., Schwegler, E. (2014). Multiphase equation of state for carbon addressing high pressures and temperatures. *Physical Review B*, *89*, 224109.

Bilgram, J. H. (1987). Dynamics at the solid-liquid transition: Experiments at the freezing point. *Physics Reports*, *153*(1), 1-89.

Blöchl, P. E. (1994). Projector augmented-wave method. *Physical Review B*, *50*, 17953-17979.

Bundy, F. P. (1980). The p, t phase and reaction diagram for elemental carbon, 1979. *Journal of Geophysical Research: Solid Earth*, *85*(B12), 6930-6936.

Chakravarty, C., Debenedetti, P. G., Stillinger, F. H. (2007). Lindemann measures for the solid-liquid phase transition. *The Journal of Chemical Physics*, *126*(20), 204508.

Cogollo-Olivo, B. H. (2020). *Phase stability of carbon, oxygen and carbon dioxide under extreme p-t conditions, beyond the harmonic approximation* (Ph. D. Thesis). Universidad de Cartagena.

Cogollo-Olivo, B. H., Biswas, S., Scandolo, S., Montoya, J. A. (2018). Phase diagram of oxygen at extreme pressure and temperature conditions: An ab initio study. *Physical Review B*, *98*(9), 094103.

Cogollo-Olivo, B. H., Biswas, S., Scandolo, S., Montoya, J. A. (2020). Ab initio determination of the phase diagram of co_2 at high pressures and temperatures. *Physical Review Letters*, *124*(9), 095701.

Correa, A. A., Benedict, L. X., Young, D. A., Schwegler, E., Bonev, S. A. (2008). First-principles multiphase equation of state of carbon under extreme conditions. *Physical Review B*, *78*, 024101.

Correa, A. A., Bonev, S. A., Galli, G. (2006). Carbon under extreme conditions: Phase boundaries and electronic properties from first-principles theory. *Proceedings of the National Academy of Sciences*, *103*(5), 1204-1208.

Crespo, Y., Fabrizio, M., Scandolo, S., Tosatti, E. (2014). Collective spin 1 singlet phase in high-pressure oxygen. *Proceedings of the National Academy of Sciences*, *111*(29), 10427–10432.

Duan, D., Liu, Z., Lin, Z., Song, H., Xie, H., Cui, T., Pickard, C.J., Miao, M. (2021). Multistep dissociation of fluorine molecules under extreme compression. *Physical Review Letters*, *126,* 225704.

Dubrovinskaia, N., Dubrovinsky, L., Solopova, N. A., Abakumov, A., Turner, S., Hanfland, M., Bykova, E., Bykov, M., Prescher C., Prakapenka, V.B., Petitgirard, S., Chuvashova, I., Gasharova, B., Mathis, Y.L., Ershov, P., Snigireva I., Snigirev, A. (2016). Terapascal static pressure generation with ultrahigh yield strength nanodiamond. *Science Advances*, *2*(7), e1600341.

Dubrovinsky, L., Dubrovinskaia, N., Bykova, E., Bykov, M., Prakapenka, V., Prescher, C., K Glazyrin K., Liermann H-P., Hanfland M., Ekholm M., Feng Q., Pourovskii L.V., Katsnelson M.I., Wills J.M., Abrikosov, I. A. (2015). The most incompressible metal osmium at static pressures above 750 gigapascals. *Nature*, *525*(7568), 226-229.

Giannozzi, P., Andreussi, O., Brumme, T., Bunau, O., Buongiorno Nardelli, M., Calandra, M., Car, R., Cavazzoni, C., Ceresoli, D., Coccoccioni, M., Colonna, N., Carnemeo, I., DalCorso, A., deGironcoli, S., Delugas, P., DiStasio, R.A., Ferretti, a., Floris, A., Fratesi, G., Fugallo, G., . . . Baroni, S. (2017). Advanced capabilities for materials modelling with quantum espresso. *Journal of Physics: Condensed Matter*, *29*, 465901.

Giannozzi, P., Baroni, S., Bonini, N., Calandra, M., Car, R., Cavazzoni, C., Ceresoli D., Chiarotti G.L., Cococcioni M., Dabo I., Corso A.D., deGironcoli S., Fabris S., Fratesi G., Gebauer R., Gerstmann U., Gougoussis C., Kokalj A., Lazzeri M., Martin-Samos L., . . . Wentzcovitch, R. M. (2009). Quantum espresso: A modular and open-source software project for

quantum simulations of materials. *Journal of Physics: Condensed Matter*, *21*, 21832390.

Gilvarry, J. J. (1956). The lindemann and graneisen laws. *Physical Review*, *102*, 2.

Goncharenko, I. N., Makarova, O. L., Ulivi, L. (2004). Direct determination of the magnetic structure of the delta phase of oxygen. *Physical Review Letters*, *93*(5), 055502.

Goncharov, A. F., Montoya, J. A., Subramanian, N., Struzhkin, V. V., Kolesnikov, A., Somayazulu, M., Hemley, R. J. (2009). Laser heating in diamond anvil cells: developments in pulsed and continuous techniques. *Journal of Synchrotron Radiation*, *16*(6), 769-772.

Goncharov, A. F., Subramanian, N., Ravindran, T. R., Somayazulu, M., Prakapenka, V. B., Hemley, R. J. (2011). Polymorphism of dense, hot oxygen. *Journal of Chemical Physics*, *135*(8), 84512.

Gorelli, F., Santoro, M., Ulivi, L., Hanfland, M. (2002). Crystal structure of solid oxygen at high pressure and low temperature. *Physical Review B*, *65*(17), 172106.

Grumbach, M. P., Martin, R. M. (1996). Phase diagram of carbon at high pressures and temperatures. *Physical Review B*, *54*, 15730-15741.

Grüneisen, E. (1926). Zustand des festen ko¨rpers. In C. Drucker et al. (Eds.), *Thermische eigenschaften der stoffe* (pp. 1–59).

Hunter, L. (1942). The variation with temperature of the principal elastic moduli of nacl near the melting point. *Physical Review*, *61*, 84-90.

Leibfried, G., Ludwig, W. (1961). Theory of anharmonic effects in crystals. *Reviews in Mineralogy and Geochemistry*, *12*(C), 275-444.

Lindemann, F. A. (1910). Ueber die berechnung molekularer eigenfrequenzen. *Physikalis- che Zeitschrift*, *11*, 609-612.

Loveday, J. (2012). *High-pressure physics*. Chapman Hall.

Löwen, H. (1994). Melting, freezing and colloidal suspensions. *Physics Reports*, *237*(5), 249-324.

Ma, Y., Oganov, A. R., Glass, C. W. (2007). Structure of the metallic ζ -phase of oxygen and isosymmetric nature of the ε-ζ phase transition: Ab initio simulations. *Physical Review B*, *76*(6), 064101.

Martinez-Canales, M., Pickard, C. J., Needs, R. J. (2012). Thermodynamically stable phases of carbon at multiterapascal pressures. *Physical Review Letters*, *108*, 045704.

Montoya, J. A., Goncharov, A. F. (2012). Finite element calculations of the time dependent thermal fluxes in the laser-heated diamond anvil cell. *Journal of Applied Physics*, *111*(11), 112617.

Murray, C. A., Grier, D. G. (1996). Video microscoopy of monodisperse colloidal systems. *Annual Review of Physical Chemistry*, *47*(1), 421-462.

Nicol, M., Hirsch, K. R., Holzapfel, W. B. (1979). Oxygen phase equilibria near 298 k. *Chemical Physics Letters*, *68*(1), 49-52.

Ohnesorge, R., Löwen, H., Wagner, H. (1993). Density distribution in a hard-sphere crystal. *Europhysics Letters*, *22*(4), 245.

Olson, M. A., Bhatia, S., Larson, P., Militzer, B. (2020). Prediction of chlorine and fluorine crystal structures at high pressure using symmetry driven structure search with geometric constraints. *The Journal of Chemical Physics*, *153*(9), 094111.

Pack, J. D., Monkhorst, H. J. (1977). Special points for brillouin-zone integrations. *Physical Review B*, *16*, 1748-1749.

Pal, S., Sharma, P. K. (1967). On lindemann's melting criterion. *Physica Status Solidi B*, *23*(1), 361-364.

Perdew, J. P., Burke, K., Ernzerhof, M. (1996). Generalized gradient approximation made simple. *Physical Review Letters*, *77*, 3865-3868.

Robinson, D. R., Wilson, M. (2013). The liquid←→amorphous transition and the high pressure phase diagram of carbon. *Journal of Physics: Condensed Matter*, *25*(15), 155101.

Ross, M. (1969). Generalized lindemann melting law. *Physical Review*, *184*, 1.

Ross, M. (1981). Polymorphism of dense, hot oxygen. *Nature*, *292*(5822), 435-436.

Santoro, M., Hajeb, A., Gorelli, F. A. (2020). Resistively heated, high pressure, membrane and screw driven diamond anvil cell. *High Pressure Research*, *40*(3), 379-391.

Schiferl, D., Cromer, D.T., Schwalbe, L.A., Mills, R.L. (1983). Structure of 'orange'18o_2 at 9.6 gpa and 297 k. *Acta Crystallographica Section B*, *39*(39), 153-157.

Schöttler, M., French, M., Cebulla, D., Redmer, R. (2016). Free energy model for solid high-pressure phases of carbon. *Journal of Physics: Condensed Matter*, *28*(14), 145401.

Smith, R.F., Eggert, J.H., Jeanloz, R., Duffy, T.S., Braun, D.G., Patterson, J.R., Rudd, R.E., Biener, J., Lazicki, A.E., Hamza, A.V., Wang J., Braun, T., Benedict, L.X., Celliers, P.M.,

Collins, G.W. (2014). Ramp compression of diamond to five terapascals. *Nature*, *511*, 330-333.

Somayazulu, M., Ahart, M., Mishra, A.K., Geballe, Z.M., Baldini, M., Meng, Y., Struzhkin, V.V., Hemley, R.J. (2019). Evidence for superconductivity above 260 k in lanthanum superhydride at megabar pressures. *Physical Review Letters*, *122*(2), 027001.

Stroud, D., Ashcroft, N. W. (1972). Theory of the melting of simple metals: Application to na. *Physical Review B*, *5*, 371-383.

Sun, J., Martinez-Canales, M., Klug, D.D., Pickard, C.J., Needs, R.J. (2012). Persistence and eventual demise of oxygen molecules at terapascal pressures. *Physical Review Letters*, *108*(4), 045503.

Swift, D.C., Heuze, O., Lazicki, A., Hamel, S., Benedict, L.X., Smith, R.F., McNaney, J.M., Ackland, G.J. (2022). Equation of state and strength of diamond in high-pressure ramp loading. *Physical Review B*, *105*, 014109.

Vopson, M. M., Rogers, N., Hepburn, I. (2020). The generalized lindemann melting coefficient. *Solid State Communications*, *218*, 113977.

Wang, X., Scandolo, S., Car, R. (2005). Carbon phase diagram from ab initio molecular dynamics. *Physical Review Letters*, *95*, 185701.

Weck, G., Desgreniers, S., Loubeyre, P., Mezouar, M. (2009). Single-crystal structural characterization of the metallic phase of oxygen. *Physical Review Letters*, *102*(25), 255503.

Weck, G., Loubeyre, P., Eggert, J. H., Mezouar, M., Hanfland, M. (2007). Melting line and fluid structure factor of oxygen up to 24 gpa. *Physical Review B*, *76*(5), 054121.

Young, D. A., Alder, B. J. (1974). Studies in molecular dynamics. xiii. singlet and pair distribution functions for hard-disk and hard-sphere solids. *The Journal of Chemical Physics*, *60*(4), 1254-1267.